Math 676 Project Report

Introduction

The strong form considered in step-86 is given as follows, with temperature field, u, heat source, f, initial temperature field, o_u, and temperature boundary conditions b_u.

$$\left\{\begin{array}{ll} \partial_t u - \Delta u = f & \forall (\mathbf{x}, t) \mid \mathbf{x} \in \Omega,\ t \in (0, T) \\ u = o_u & \forall (\mathbf{x}, t) \mid \mathbf{x} \in \Omega,\ t = 0 \\ u = b_u & \forall (\mathbf{x}, t) \mid \mathbf{x} \in \partial\Omega,\ t \in (0, T) \end{array}\right\}$$

In this program, we extend step-86 in order to simulate Selective Laser Sintering (SLS). SLS is an additive manufacturing technique in which a laser is directed onto the surface of a powder bed in order to selectively sinter patterns into this bed. Sufficient physical realism for modelling SLS is achieved by supplementing this model with thermal conductivity, k, thermal mass, $m = \rho c$, and degree of cohesion, θ, each of which coupled with the temperature and cohesion. Relatively simple material models are used in this program, but since the complexity of temperature and cohesion coupling is already accounted for, these models could be refined with simple changes to the parameter input files.

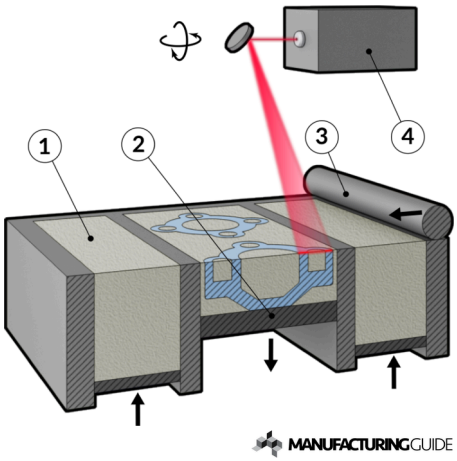

Figure 1. Selective Laser Sintering Process [1]

Strong Form Derivation

Degree of Cohesion

The rate of change of the degree of cohesion, θ, here ‘stickiness’, s, is coupled to both temperature, u, and cohesion. This is modeled based off a maximum rate, S, and made to approach 1 asymptotically by the $(1 - \theta)$ factor. Further, a sigmoidal model is used for the temperature coupling, utilizing a threshold temperature, u_t, a threshold deviance, d_t, to reflect the particle sintering at and around the melting point.

$$\partial_t \theta = s(u,\theta) = \frac{S(1-\theta)}{1+e^{-\frac{u-u_t}{d}}}$$

$$\partial_u s(u,\theta) = \frac{S(1-\theta)}{d(1+e^{-\frac{u-u_t}{d}})^2} e^{-\frac{u-u_t}{d}}$$

$$\partial_\theta s(u,\theta) = -\frac{S}{1+e^{-\frac{u-u_t}{d}}}$$

Thermal Conductivity

We model the thermal conductivity linearly. We utilize $(1-\theta)$ and (θ) factors to interpolate between the non-cohesed case and the cohesed case. In the non-cohesed case, we use a simple constant model for the equivalent conductivity of the randomly packed powder and atmosphere, k_{p0}. In the cohesed case, we use a slightly more complex model, linear with temperature, withk_{m0} and k_{m1}.

$$k(u,\theta) = (k_{p0})(1-\theta) + (k_{m0} + k_{m1}u)(\theta)$$

$$\partial_u k(u,\theta) = (k_{m1}u)(\theta)$$

$$\partial_\theta k(u,\theta) = -(k_{p0}) + (k_{m0} + k_{m1}u)$$

Thermal Mass

We use a simple constant model for the density and specific heat. However, we supplement the specific heat with a gaussian increment in order to model the latent heat of the solid to liquid transition. This increment is correspondent to threshold quantities in the cohesion model, and likewise utilizes a threshold temperature, u_t, and threshold deviance, d_t.

$$m(u,\theta) = (\rho_0)(c_0 + \frac{H}{d_t\sqrt{2\pi}} e^{-\frac{1}{2}(\frac{u-u_t}{d_t})^2})(0.6+0.4\theta)^2$$

$$\partial_u m(u,\theta) = -\rho_0 \frac{H}{d_t^3\sqrt{2\pi}}(u-u_t) e^{-\frac{1}{2}(\frac{u-u_t}{d_t})^2}(0.6+0.4\theta)^2$$

$$\partial_\theta m(u,\theta) = (\rho_0)(c_0 + \frac{H}{d_t\sqrt{2\pi}} e^{-\frac{1}{2}(\frac{u-u_t}{d_t})^2})(0.8\theta)$$

Heat Source

A bivariate gaussian distribution is used to model the laser radiation. This model uses a total power, p_l, standard deviation, d_l, trace radius, $r_t = r_0 + r_1 t$, and trace angular velocity, ω_t.

$$f(x,y) = \frac{p_l}{2\pi d_l} e^{-\frac{1}{2d_l^2}((x-r_t\cos\omega_t t)^2 + (y-r_t\sin\omega_t t)^2)}$$

Augmented Strong Form

The augmented strong form is thus consolidated as below.

$$\left\{\begin{array}{cc} m(u,\theta)\partial_t u - \nabla\cdot(k(u,\theta)\nabla u) = f & \forall(\mathbf{x},t) \mid \mathbf{x}\in\Omega,\ t\in(0,T) \\ \partial_t\theta = s(u,\theta) & \forall(\mathbf{x},t) \mid \mathbf{x}\in\Omega,\ t\in(0,T) \\ u = o_u & \forall(\mathbf{x},t) \mid \mathbf{x}\in\Omega,\ t=0 \\ \theta = o_\theta & \forall(\mathbf{x},t) \mid \mathbf{x}\in\Omega,\ t=0 \\ u = b_u & \forall(\mathbf{x},t) \mid \mathbf{x}\in\partial\Omega,\ t\in(0,T) \\ \theta = b_\theta & \forall(\mathbf{x},t) \mid \mathbf{x}\in\partial\Omega,\ t\in(0,T) \end{array}\right\}$$

Weak Form Derivation

By testing with $\varphi \in H_0^1(\Omega)$ and integrating over Ω the weak form is derived as normal.

$$\left\{\begin{matrix}(\varphi, m\partial_t u) - (\varphi, \nabla \cdot (k\nabla u)) = (\varphi, f) \\ (\varphi, \partial_t \theta) = (\varphi, s) \\ \dots \end{matrix}\right\} \quad \forall \varphi \in H_0^1(\Omega)$$

It helps to recall Green's first identity.

$$\int_\Omega \left(\phi \Delta \psi\right) d\Omega = \int_{\partial\Omega} \left(\phi \nabla \psi\right) \cdot \mathbf{n} \partial\Omega - \int_\Omega \left(\nabla \phi \cdot \nabla \psi\right) d\Omega$$

$$\left\{\begin{matrix}(\varphi, m\partial_t u) + (\nabla\varphi, k\nabla u) = (\varphi, f) + (\varphi, k\nabla u \cdot \mathbf{n}) \\ (\varphi, \partial_t \theta) = (\varphi, s) \\ \dots \end{matrix}\right\} \dots$$

Since Dirichlet boundary conditions will be used, the boundary term is eliminated.

$$\left\{\begin{matrix}(\varphi, m\partial_t u) + (\nabla\varphi, k\nabla u) = (\varphi, f) \\ (\varphi, \partial_t \theta) = (\varphi, s) \\ \dots \end{matrix}\right\} \dots$$

We select a basis for our finite element, $\text{span}(\Phi) = V \subset H_0^1(\Omega)$ and take our approximated solutions for u and θ to be linear combinations of this basis.

$$u_h = \sum u_i = \sum U_i \varphi_i \quad \theta_h = \sum \theta_i = \sum \Theta_i \varphi_i$$

Thus, we obtain the implicit weak form as follows.

$$\left\{\begin{matrix}(\varphi_i, m\partial_t u) + (\nabla\varphi_i, k\nabla u) - (\varphi_i, f) = 0 \\ (\varphi_i, \partial_t \theta) - (\varphi_i, s) = 0 \\ \dots \end{matrix}\right\} \quad \forall \varphi_i \in \Phi$$

We will utilize a finite element system in which the degrees of freedom for temperature and cohesion are interleaved. We thus obtain a residual vector as follows.

$$R_i = \begin{bmatrix}(\varphi_i, m\partial_t u) + (\nabla\varphi_i, k\nabla u) - (\varphi_i, f) \\ (\varphi_i, \partial_t \theta) - (\varphi_i, s)\end{bmatrix}$$

We also obtain an approximation of the implicit Jacobian, $J_\beta = \beta \partial_{\dot{y}} R + \partial_y R$, as follows. This is an approximation because the differentiation of m, k, s factors are simplified for the sake of tractability.

$$J_{ij}^\beta = \begin{bmatrix}\beta(\varphi_i, m\varphi_j) & 0 \\ 0 & \beta(\varphi_i, \varphi_j)\end{bmatrix} + \begin{bmatrix}(\varphi_i, \partial_t u_j \, \partial_u m \varphi_j) & (\varphi_i, \partial_t u_j \, \partial_\theta m \varphi_j) \\ 0 & 0\end{bmatrix} + \begin{bmatrix}(\nabla\varphi_i, k\nabla\varphi_j) + (\nabla\varphi_i, \nabla u_j \, \partial_u k \varphi_j) & (\nabla\varphi_i, \nabla u_j \, \partial_\theta k \varphi_j) \\ 0 & 0\end{bmatrix} + \begin{bmatrix}0 & 0 \\ -(\varphi_i, \partial_u s \varphi_j) & -(\varphi_i, \partial_\theta s \varphi_j)\end{bmatrix}$$

Commented Code

Rather than copy the code into this report and lose syntax highlighting, the comments have simply been included in `step-86.cc`. These comments focus on how the program was modified from the original tutorial step.

Results

Convergence Testing

We may recall the strong form of the problem for the sake of designing manufactured solutions.

$$\left\{\begin{array}{c} m(u,\theta)\partial_t u - \nabla\cdot(k(u,\theta)\nabla u) = f \\ \partial_t \theta = s(u,\theta) \end{array}\right\}$$

We then assert our manufactured solutions to obtain the necessary source functions.

$$u = e^{-t}\cos\left(\tfrac{\pi}{2r^2}(x^2+y^2)\right),\ \theta = e^{-t}\cos\left(\tfrac{\pi}{2r^2}(x^2+y^2)\right),\ m = u\theta,\ k = u\theta \Rightarrow$$

$$s = -\frac{1}{2}(u+\theta)$$

$$f = e^{-3t}(-\cos^3(\psi) - 2\cos(\psi)\sin^2(\psi)\frac{\pi^2}{r^4}(x^2+y^2) + \cos^3(\psi)\frac{\pi^2}{r^4}(x^2+y^2) + 2\cos^2(\psi)\sin(\psi)\frac{\pi}{r^2}), \psi = \frac{\pi}{2r^2}(x^2+y^2)$$

Using this manufactured solution, convergence was tabulated as follows.

Refinement	L^2	Convergence
1	0.9377	-
2	0.3142	1.5772
3	0.0830	1.9206
4	0.0431	0.9458
5	0.0656	-0.6067

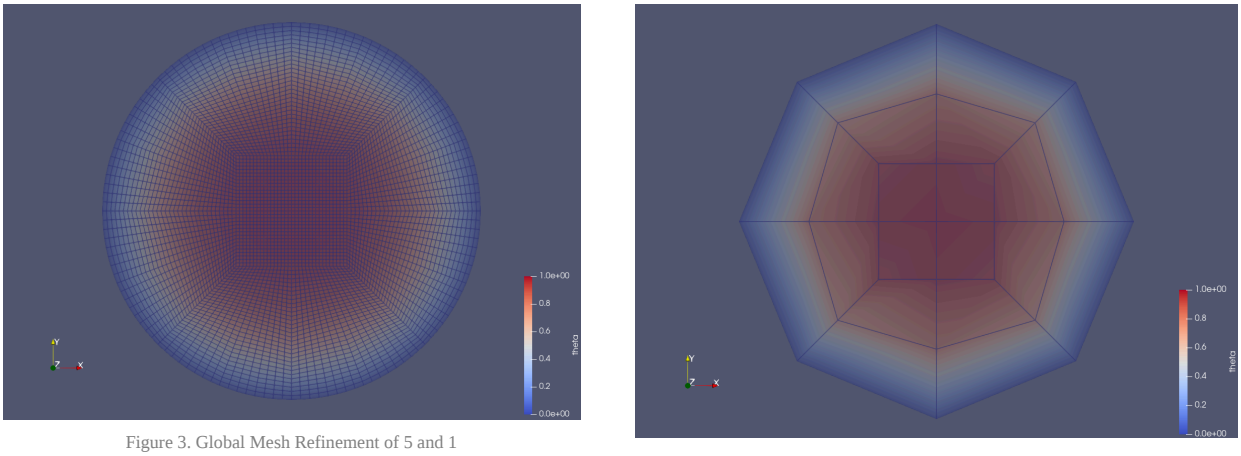

Figure 3. Global Mesh Refinement of 5 and 1

As shown, the convergence plateued around a mesh refinement of 4. At mesh refinements at 5 and beyond, the number of linear steps increased dramatically, exceeding 200 (though nonlinear steps remained constant at about 5). Unfortunately, the cause of this failure to converge was not identified.

Another major issue identified was that enabling mesh refinement dramatically increased the number of non-linear steps at each time step. For this reason, adaptive mesh refinement was effectively disable in all parameter files by setting maximum delta refinement level to zero.

Realistic Selective Laser Sintering Demo

Following is a demo of the realistic simulation, with the modeling detailed in the introduction.

Temperature Field: https://youtu.be/03S2POnLToU

https://youtu.be/03S2POnLToU

Cohesion Field: https://youtu.be/qUMs9oG6tjM

https://youtu.be/qUMs9oG6tjM

References

[1] Manufacturing Guide, Selective Laser Sintering, https://www.manufacturingguide.com/en/selective-laser-sintering-sls